

The Development of a Micro-Fabricated CNT-Based Neutralizer for Micro-Propulsion Applications

Luis Fernando Velásquez-García*
Massachusetts Institute of Technology, Cambridge, MA 02139 USA

This paper reports the preliminary development of a micro- and nano-fabricated carbon nanotube (CNT) –based electron source intended for micro-propulsion applications. The paper proposes a device that implements a trade-off between microfabrication complexity and performance using a 3D packaging technology to minimize interception and decouple the process flows of the grid and the emitter array. The device uses plasma enhanced chemical vapor deposited (PECVD) CNTs as field enhancers. The PECVD CNT growth is documented, and IV characteristics of the emitted current from a micro-/nano-structured emitter substrate are provided. A maximum emitted current of 71 μA @ 480 V is obtained from a 0.25 cm^2 estimated active emitter area and a grid with 200 μm separated 50 μm from the emitters. The electron source emission can be described by the Fowler-Nordheim theory, and a field enhancement of $3.69 \times 10^5/\text{cm}$ –corresponding to an emitter tip radius of 27 nm.

Nomenclature

A	=	emitted current proportionality constant
α	=	effective emitter area
B	=	image charge effect correction proportionality constant
β	=	field factor
ϕ	=	work function
I_{TIP}	=	Emitter (tip) current
k	=	field factor proportionality constant
n	=	power dependence of field factor on tip radius
r	=	tip radius
V_G	=	bias gate voltage

I. Introduction

THE majority of electric rockets such as ion engines and hall thrusters emit a stream of positive charged particles to produce thrust.¹ In the case of electrospray propulsion² it is possible to implement an engine that produces thrust by emitting charged particles of both polarities.³ For the other cases, a suitable source of opposite polarity current is needed to keep the overall spacecraft charge neutrality, i.e., a neutralizer. The most widely neutralizer implementation is a hollow cathode, where a noble gas plasma is produced and electrons are extracted from it using a biased grid.⁴ Even though hollow cathodes are very efficient, in some micro-propulsion applications, in particular missions that involve the use of FEEPs⁵ and electrospray thrusters, hollow cathodes are unattractive because they would introduce prohibitive mass flowrate expenses compared to the engine mass flowrate that is used to produce thrust. Instead, low-power, low-voltage, efficient field emission neutralizers are a more adequate choice.

Electrons are field emitted from the surface of metals and semiconductors when the potential barrier (work function ϕ) that holds electrons within the metal or semiconductor is deformed by the application of a high electrostatic field. The application of the field allows electrons to tunnel into vacuum. The probability of electron tunneling becomes significant when the barrier width is of the order of several electron wavelengths. The typical barrier width at which electron tunneling occurs is about 1.5 nanometers while the corresponding typical barrier height is 4.5 eV. Hence, for electron tunneling to occur the surface electrostatic field has to be about 3.0 V/nm assuming a linear potential distribution at the surface. Field emitters use high aspect ratio structures with tips that

* Research Scientist, Microsystems Technologies Laboratories, Massachusetts Institute of Technology, 77 Massachusetts Avenue 39-657, Cambridge MA USA, not an AIAA Member.

have nanometer dimensions to generate very high fields even when low voltages are applied. Some other researchers have proposed field emission structures that use other materials such as boron nitride.⁶ However, the ideal field enhancing structure would be a rounded whisker –the shape of a CNT.⁷

The two most important parameters that determine field emission current density are the work function –which determines the barrier height, and the tip radius r –which determines the barrier width. If the emitter tip radius is far smaller than the emitter height, the field factor β is defined as

$$\beta = \frac{k}{r^n} \quad (1)$$

where k is a proportional constant and n is a positive number between 0.6 and 1.0. The field factor is a direct measure of the field enhancement capabilities of the emitter. The field factor has units of length^{-1} . The field factor times the bias voltage V_G is equal to the electric field at the surface of the emitter.

The Fowler – Nordheim (FN) equation relates the current density to the electrostatic field and the work function. The emitted current I_{TIP} is given by

$$I_{TIP} = \frac{\alpha A \left(\frac{k}{r^n} \right)^2}{1.1\phi} \exp \left[\frac{B(1.44 * 10^{-7})}{\phi^{1/2}} \right] \times V_G^2 \times \exp \left[-\frac{0.95 B \phi^{3/2} r^n}{k V_G} \right] \quad (2)$$

where A and B are constants and α is the effective emitter area. The adoption of CNTs as electron-emitting structure has recently been shown to pose advantages compared to silicon-based⁸ and metal-based⁹ emitters because of the higher aspect ratio of the CNTs, and their superior resistance to harsh environments, in particular to the presence of oxygen –the case of the atmosphere present in LEO.¹⁰

The implementation of micro- and nano-fabrication technologies would allow us to produce devices with smaller starting voltages, better area usage, and more uniform I – V characteristics, compared to macro/meso fabricated field emitter versions. Also, a MEMS neutralizer is batch fabricated. Many devices can be then mass-produced at a fraction of the cost and time, thus enabling the implementation of missions with dense nanosatellite constellations.¹¹

II. Device Concept

A MEMS neutralizer should represent a trade-off between device performance and fabrication complexity. There are two key ideas to take into account while making this trade-off. First, emitter shadowing should be avoided to be able to take advantage of the remarkable field enhancement properties of CNTs. Unfortunately, a forest of PECVD CNTs usually has CNT pitch of the order of a fraction of a micrometer (see Section III). Therefore, a neutralizer that uses CNT forests would probably need larger bias voltages to achieve the same current, and in any case only a small fraction of the CNTs will actually be emitting. There has been recently reported work on implementing CNT-based field emitter arrays, particularly focusing on isolated CNTs.¹² Figure 1 shows an array of isolated PECVD CNTs grown in our reactor, using electron beam nanophotolithography and lift-off to define the catalyst dots (nickel). There are some drawbacks with using these micro- and nano-fabrication techniques such as throughput and cost because electron beam nanophotolithography defines one catalyst dot at a time. The use of a micro-structured surface that is defined using contact photolithography and reactive ion etching (RIE) to reduce emitter shadowing would be a more effective solution. The catalyst would be deposited everywhere on the micro-structured surface and a PECVD CNT forest would then be grown. The non-flatness of the surface will produce CNT clusters or islands, thus decreasing the emitter shadowing (Fig. 2). The islands would be spaced twice the CNT height to maximize field enhancement. The trench depth should be at least of the same order of the CNT height. RIE is a good option to etch in silicon a depth of the order of the height of what our CNT reactor can grow (around ten μm).

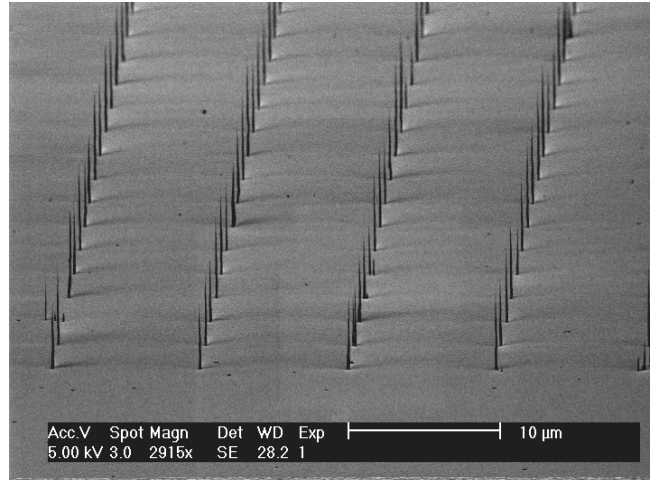


Figure1. An array of isolated PECVD CNTs 6 μm tall spaced 10 μm .

The second issue to take into account is the neutralizer gate. Macro-fabricated stretched metallic meshes have been successfully implemented in CNT neutralizers¹⁰; however, this approach does not allow batch fabrication. Deep Reactive Ion Etched (DRIE) gates can be used instead. The grids can implement a 3D packaging system¹³ that has micron resolution and alignment capability of the order of a few microns¹⁴. The electrical insulation can be directly provided by micro-fabrication processing, or by the use of dielectric gaskets. We have successfully used 1-mil and 2-mil polymer and mica gaskets from Mc Master (Robbinsville, NJ) in devices biased up to 1100 DC V. For a 1-mil to 2-mil spacer, a silicon grid with holes of the same size can readily be patterned with aspect ratios as large as 25 (Fig. 3). Given the fact that the proposed 3D packaging system has micron-level repeatability, it is possible to use the grid as a shadow mask to deposit the catalyst to reduce the gate current interception (reduction of CNTs directly below the grid). PECVD CNTs can be then grown on the emitter substrate, to later be assembled to the previous grid and have to first order a self-aligned structure (emitters concentric to the grid apertures). The small variations in DRIE batch processing would allow us to use dedicated grids for the catalyst definition into the emitter substrate.

The proposed MEMS neutralizer is shown in Fig. 4. An schematic is included to provide further insights into its structure.

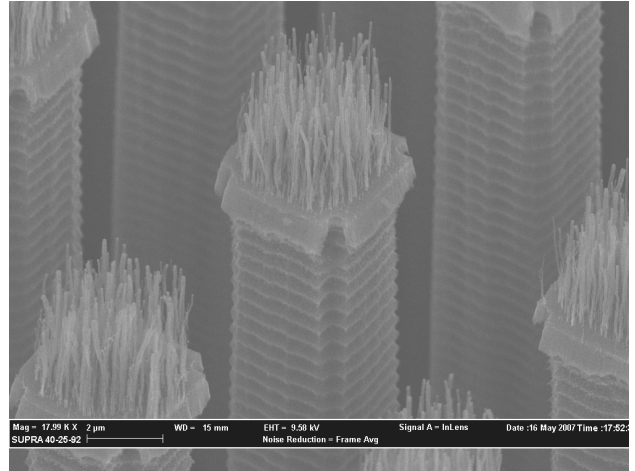


Figure2. A n-Si patterned substrate to produce islands of CNTs. The CNTs are 5 μm tall spaced 10 μm . The minimum trench depth needed is about the CNT height.

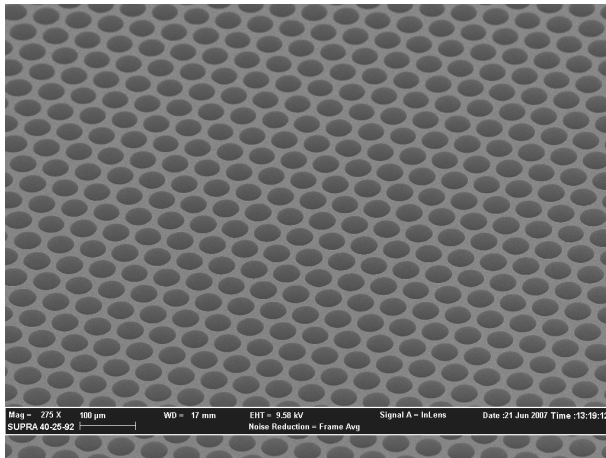


Figure3. A microstructured grid patterned with DRIE. Maximum field enhancement is obtained if the grid holes are of the same size of the emitter to gate separation.

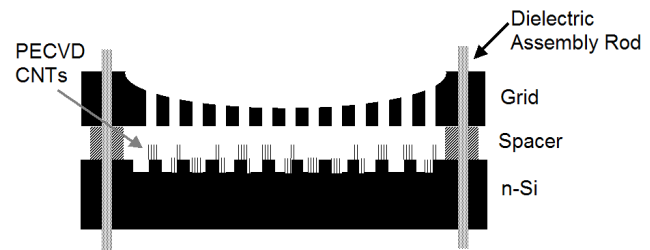
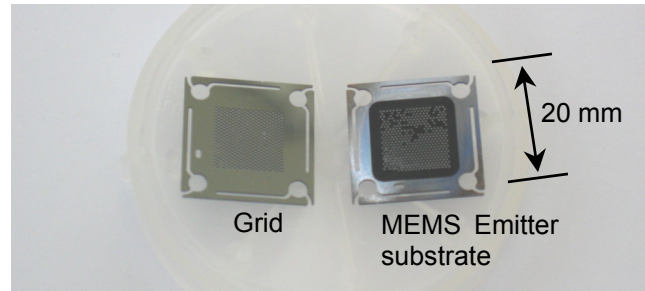


Figure4. A disassembled micro- and nano-fabricated neutralizer (top) and schematic of device structure (bottom). The grid and emitter substrate includes deflection springs for assembly. The dielectric assembly rods interact with the springs.

III. PECVD CNT growth Characterization

To grow PECVD CNTs we use an acetylene/ammonia mix to obtain tall graphite nanotubes and minimize the growth of other allotropic forms of carbon. In general, there are two key steps to grow CNT forests: the generation

of catalyst seeds (nanospheres) by reduction of the catalyst metal at high temperature on top of a non-wetting surface, and the generation of plasma rich of carbon-based radicals to supply the seeds with the raw materials for graphite growth. In PECVD CNT growth the nanospheres absorb the carbon radicals present on the plasma; the concentration of carbon supersaturates within the nanosphere until it precipitates, thus forming a seamless graphite tube using as template the catalyst seed. In PECVD CNT growth the catalyst seed remains on top of the CNT. The following is a brief experimental sampling of the capabilities of our PECVD CNT reactor –an improved version of the Cambridge University (UK) reactor¹⁵, addressing these two key steps.

A. Catalyst seed formation

Figure 5 shows a set of SEMs of the typical CNT catalyst seeds formed in our reactor. In all cases the catalyst is Nickel on top of TiN and the reducing atmosphere is ammonia. Thicker films require longer reduction time (Fig. 5-a) and thicker films generate larger nanospheres (Fig. 5-b, Fig. 5-c). Longer annealing time generates thinner nanospheres at the expense of larger dimensional variation (Fig. 5 –d, Fig. 5-e). Higher annealing temperatures also reduce the nanosphere size but it can also worsen the size variation if the catalyst is annealed too long (Fig.5-f)

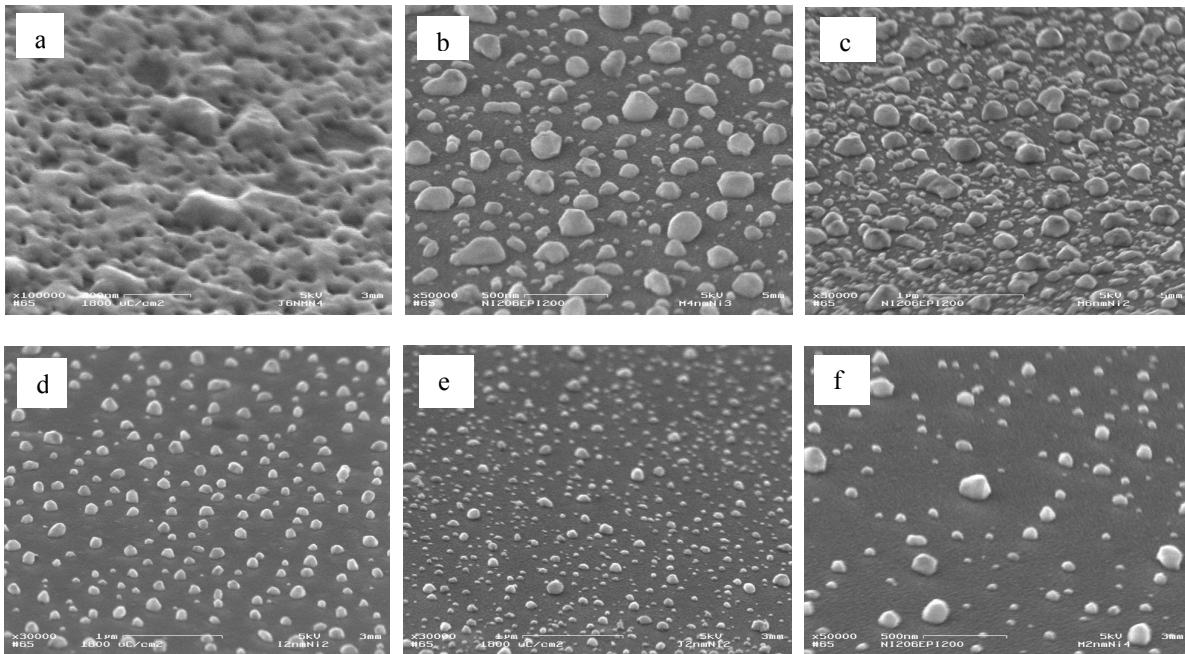


Figure5. Selected samples of CNT catalyst seed formation. 6 nm Ni, 650 °C, and 20 minutes annealing time (a); 4 nm Ni, 700 °C, and 20 minutes annealing time (b); 6 nm Ni, 700 °C, and 20 minutes annealing time (c); 2 nm Ni, 650 °C, and 15 minutes annealing time (d); 2 nm Ni, 650 °C, and 20 minutes annealing time (e); 2 nm Ni, 700 °C, and 20 minutes annealing time (f).

B. PECVD CNT Growth

Figure 6 shows a set of pictures that illustrate the typical CNT forests grown in our reactor. PECVD allows us to grow vertically aligned CNTs firmly attached to the substrate, thus enabling the fabrication of electrical devices. In all cases the plasma bias was set between 600 V and 680 V DC, and 90 to 150 W of plasma power. For a given catalyst thickness there is roughly a linear relationship between growth time and CNT length –until the CNT seed is poisoned and/or the CNT growth reached saturation. The reactor is able to grow down to 1 μm tall CNTs (Fig. 6-a), to 14 μm tall or more (Fig. 6-b). The catalyst is at the top of the CNT (Fig. 6-C), and the typical CNT tip radius for CNT forests is tens of nanometers (Fig. 6-d). This aspect ratio is very attractive for field emission applications.

IV. Experimental Data and Discussion

A micro-structured emitter substrate with a PECVD CNT forest from filed deposited nickel catalyst was tested in a triode configuration, as shown in Fig. 6. The vacuum was kept at 10⁻⁹ Torr, and Keithley 237 Voltage/ Current source-measure units were used to bias voltages and measure the gate, anode and emitter currents. The current

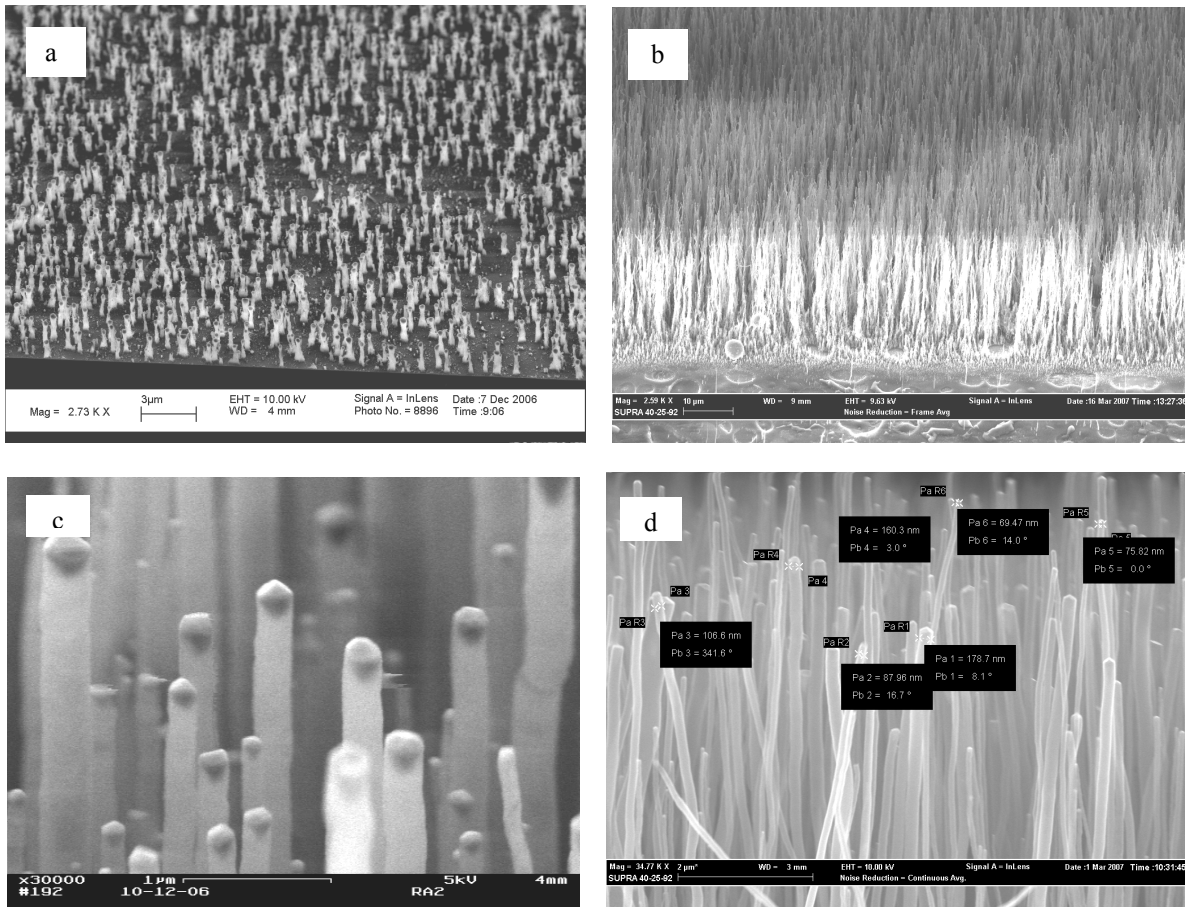


Figure 5. Selected samples of PECVD CNT growth. 7 nm Ni, 656 °C, and 20 minutes growth time (a); 15 nm Ni, 825 °C, and 80 minutes growth time (b); 7 nm Ni, 8250 °C, and 20 minutes growth me (c); 7 nm Ni, 825 °C, and 30 minutes growth time (d).

measurement error was less than 10^{-12} A and the voltage error was less than $10\mu\text{V}$. In all cases it was verified that the emitter current was equal to the gate current plus the anode current. The emitter substrate was tested using a DRIE-patterned silicon grid with $200\ \mu\text{m}$ holes spaced $400\ \mu\text{m}$, coated with sputtered metal. The grid did not include the proposed spring system. A dielectric spacer $50\ \mu\text{m}$ thick was used as electrical insulation.

The purpose of the experimentation was to demonstrate Fowler-Nordheim field emission, and to get an estimate of the field enhancement properties of the emitters. It is expected that lowers voltages would be required to produce similar current levels in an integrated device that uses thinner spacers and denser gate grids because of the closer proximity of the gate to the emitters.

Figure 7 shows in semi log scale the data collected sweeping 9 times the 0 – 480 V range in steps of 2 V. Each data point of all sweeps results from averaging 32 measurements. All the measurements were carried out automatically using the commercial software Labview. Electron emission occurs at about 150 V (1nA). The gate current is far larger than the anode current, as expected from using an un-optimized grid and spacer. The parallelism of the two

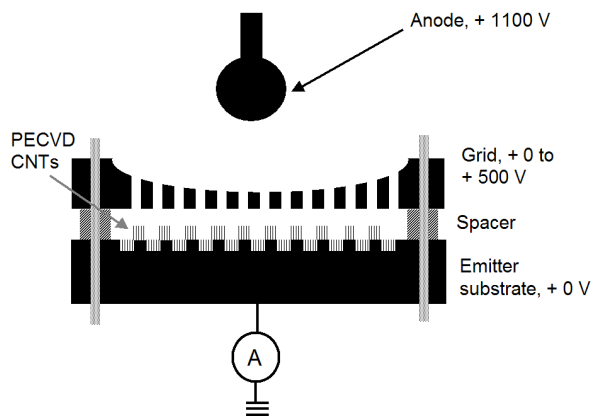


Figure 6. Schematic of the triode structure to test the field enhancement capabilities of the micro-structured PECVD CNT emitter substrate.

IV Characteristics MEMS Emitter Substrate

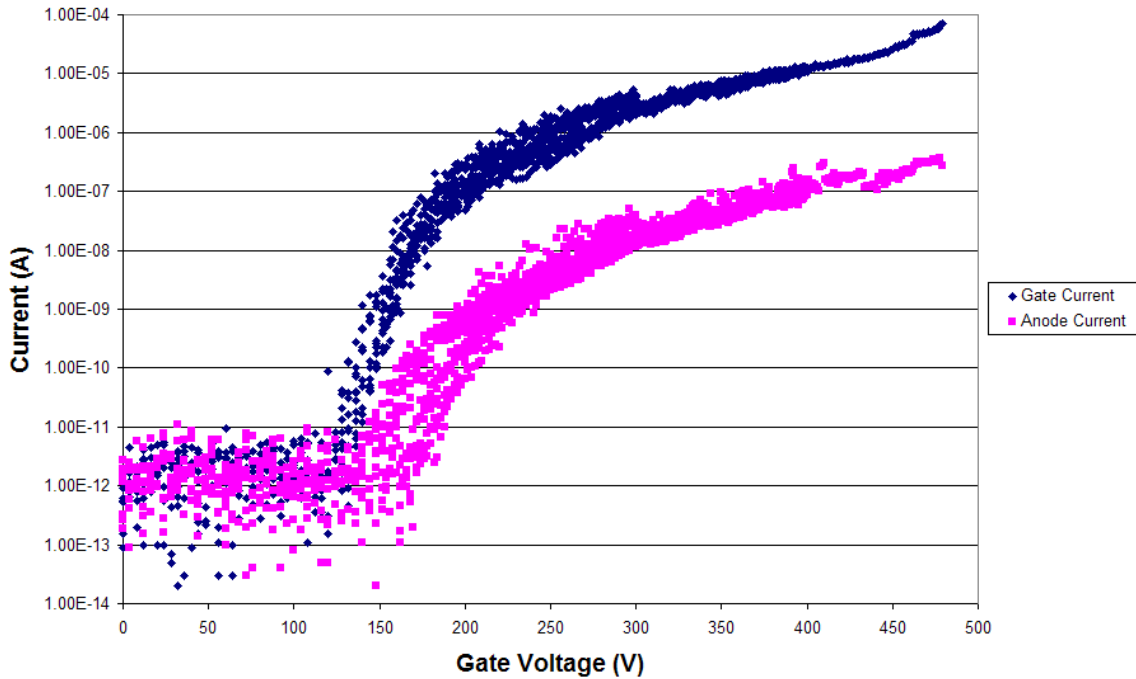


Figure 7. I-V characterization of the micro- and nano-structured emitter substrate using the triode configuration shown in Fig. 6.

current curves means that that the two currents come from the same source, and that the gate transmission is maintained over the experiment (no substantial reflow of the spacer). As a matter of fact, if the anode current vs. the gate current is plotted (Fig. 8), a linear relationship is obtained. This further corroborates that the gate and anode currents come from the same source, i.e., that the gate current does not come from leaking of the spacer but from the

Anode Current vs Gate Current

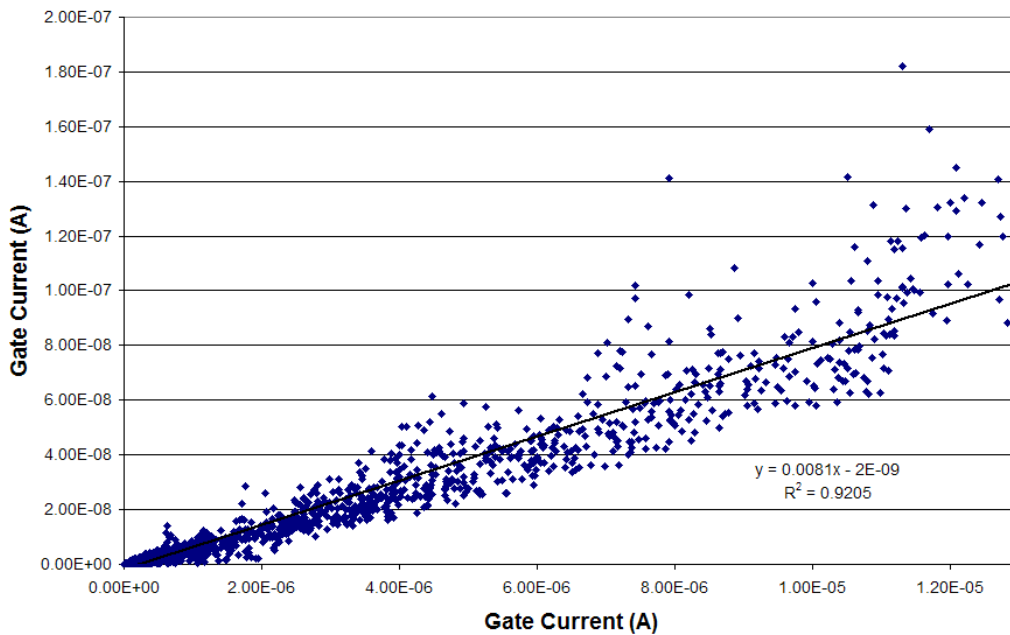


Figure 8. Anode current vs. gate current. The linear relationship between the two currents evidences the common source of the gate and anode currents.

emission of the emitters.

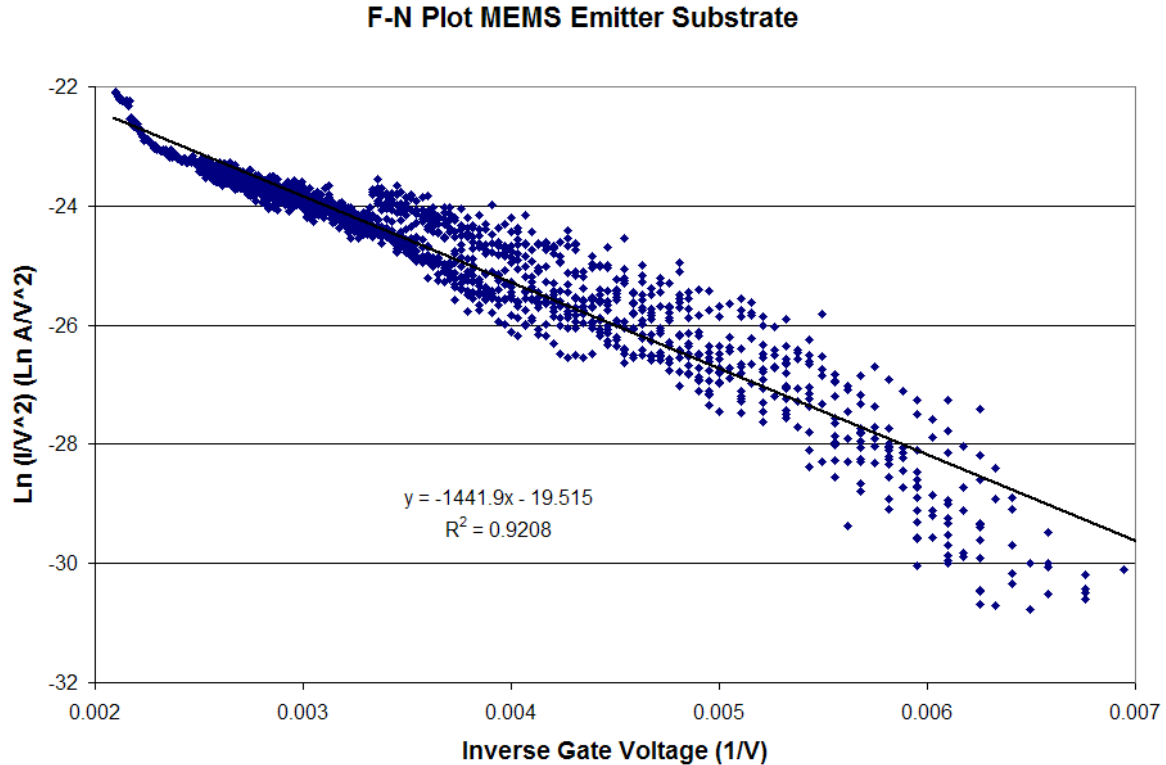


Figure 9. Fowler-Nordheim plot of the data. *The plot demonstrates that the current is field emitted.*

Finally, a Fowler-Nordheim plot of the data evidences that the substrate field emits (Fig. 9). The slope of the Fowler-Nordheim plot is 1441.9, which implies for the material properties of carbon a field enhancement of $3.69 \times 10^5/\text{cm}$. If Eq. (1) is used with $k = 1$, $n = 1$, then emitter radii of 27 nm is obtained, in good agreement with the SEM metrology of the CNTs.

V. Conclusion and Future Work

A MEMS neutralizer that uses PECVD CNT emitters is proposed. The device implements a trade-off between fabrication complexity and performance. The device uses a 3D packaging technology that augments device yield and enables decoupling of the process flows of the subsystems. CNT catalyst formation and PECVD CNT growth is characterized. Triode experimental characterization demonstrates the electron emission is described by the Fowler-Nordheim model. Field enhancement factors of $3.69 \times 10^5/\text{cm}$ are obtained, corresponding to emitter tip radius of 27 nm, in agreement with the metrology of the CNT tips from SEMs. Future work includes integration of the MEMS grid, and the implementation of shadow mask deposition to decrease the gate current interception. Finally, MEMS neutralizers might be able to emit large enough current at a low enough voltage to become an efficient neutralizer for larger electric thrusters such as low power Hall thrusters and ion engines. Some ballasting mechanism would probably be needed to improve the current density uniformity and the overall emitted current.¹⁶

Acknowledgments

The author would like to thank Professor A. I. Akinwande for his support in conducting this research, and for the fruitful discussions that we had on field emission and CNT-based devices. The author would also like to thank Mr. B. Andeoti and Dr. L-Y. Chen for his help in assisting the PECVD reactor and taking some of the SEM pictures. The author would like to acknowledge the invaluable help of the staff of MIT's Microsystems Technology Laboratories during the microfabrication of the devices. The work reported in this paper was sponsored by DARPA/MTO and the US Army Soldier Systems Center (Natick, MA) through contract # W911QY-05-1-0002 (DARPA program manager Dennis Polla, and Army program manager Henry Girolamo). The views and conclusions

contained in this document are those of the authors and should not be interpreted as representing the official policies, either expressed or implied, of the Defense Advanced Research Projects Agency or the U.S. Government.

References

- ¹Sutton, G. P., "Rocket Propulsion Elements," 7th ed., John Wiley & Sons, New York, 2001, Chapter 19.
- ²Gamero, M., Hruby, V., "Electrospray as a Source of Nanoparticles for Efficient Colloid Thrusters, *Journal of Propulsion and Power*, Vol. 17 No. 5, 2001, pp. 977-987.
- ³Mahoney, J. F., Moore, R. D., Perel, J., Yahiku, A., "Research and Development of a Charged-Particle Bipolar Thruster," *AIAA Journal*, Vol. 7, No. 3, 1969, pp. 507-511.
- ⁴Kameyama, I., and Wilbur, P., "Measurements of Ions from High Current Hollow Cathodes Using Electrostatic Energy Analyzer", *Journal of Propulsion and Power*, Vol. 16, No 3, 2000, pp. 529-535
- ⁵Tajmar, M., Genovese, A., and Steiger, W., "Indium Field Emission Propulsion Micro-thruster Experimental Characterization," *Journal of Propulsion and Power*, Vol. 20 No. 2, 2004, pp. 211-218.
- ⁶Goldberg, H., Encarnación, P., Morris, D., Gilchrist, B., and Clarke, R., "Cold-Cathode Electron Field Emission of Boron Nitride Thin Film with a MEMS-based Gate for Space Applications," AIAA-2004-3499, 40th AIAA/ASME/SAE/ASEE Joint Propulsion Conference and Exhibit, Fort Lauderdale, Florida, July 11-14, 2004.
- ⁷Utsumi, T., "Vacuum microelectronics: What's new and exciting," *IEEE Transactions on Electron Devices*, Vol. 38, No. 10, 1991, pp. 2276-2283.
- ⁸Itoh, J., Tohma, J., Morikawa, K., Kanemaru, S., and Shimizu, K., "Fabrication of double-gated Si field emitter arrays for focused electron beam generation," *Journal of Vacuum Science and Technology B*, Vol. 13, No. 5, 1995, pp. 1968-1972.
- ⁹Spindt, C. A., Brodie, I., Humphrey, L., and Westerberg, E. R., "Physical properties of thin-film field emission cathodes with molybdenum cones," *J. Appl. Phys.*, Vol. 47, No. 12, 1976, pp. 5248-5263.
- ¹⁰Gadaska, C., Falkos, P., Robin, M., Hruby, V., Demmons, N., and McCormick, M., "Testing Carbon Nanotube Field Emission Cathodes," AIAA-2004-3427, 40th AIAA/ASME/SAE/ASEE Joint Propulsion Conference and Exhibit, Fort Lauderdale, Florida, July 11-14, 2004.
- ¹¹Mueller, J., "Thruster Options for Micro-spacecraft – A Review and Evaluation of Existing Hardware and Emerging Technologies," AIAA-1997-3058, 33rd AIAA/ASME/SAE/ASEE Joint Propulsion Conference and Exhibit, Seattle, Washington, July 6-9, 1997.
- ¹²Chen, L.-Y., Velásquez-García, L. F, Wang, X., Cheung, K., Teo, K., and Akinwande, A. I., "Design, Fabrication and Characterization of Double-Gated Vertically Aligned Carbon Nanofiber Field Emitter Arrays", *Technical Digest of the 20th International Vacuum Nanoelectronics Conference*, Chicago II, USA July 8 - 12, 2007.
- ¹³Velásquez-García, L. F., Akinwande, A. I., and Martínez-Sánchez, M., "Precision Hand Assembly of MEMS subsystems using DRIE-patterned deflection Spring Structures: An Example of an Out-of-plane Substrate Assembly," accepted for publication, *Journal of MicroElectroMechanical Systems*, 2007.
- ¹⁴Gassend, B., Velásquez-García, L. F., Akinwande, A. I., and Martínez-Sánchez, M. "Mechanical Assembly of Electrospray Thruster Grid", IEPC 2005-101, 29th International Electric Propulsion Conference, Princeton University, October 31 – November 4, 2005.
- ¹⁵Teo, K., Lee, S-B., Chhowalla, M., Semet, V., et al, "Plasma-enhanced Chemical Vapor Deposition Carbon Nanotubes/Nanofibers – How Uniform do they grow?," *Nanotechnology*, Vol. 14, 2003, pp. 204-211.
- ¹⁶Hong, C-Y., and Akinwande, A. I., "Temporal and Spatial Current Stability of Smart Field Emission Arrays," *IEEE Transactions on Electron Devices*, Vol. 52, No. 10, 2005, pp. 2323-2328.